Journal of Molecular Catalysis B: Enzymatic 67 (2010) 21–28

Contents lists available at ScienceDirect

Journal of Molecular Catalysis B: Enzymatic

journal homepage: www.elsevier.com/locate/molcatb

Amino ester hydrolase from *Xanthomonas campestris pv. campestris*, ATCC 33913 for enzymatic synthesis of ampicillin

Janna K. Blum, Andreas S. Bommarius*

School of Chemical and Biomolecular Engineering, Parker H. Petit Institute for Bioengineering and Bioscience, Georgia Institute of Technology, 315 Ferst Drive, Atlanta, GA 30332-0363, USA

ARTICLE INFO

Article history:
Received 14 March 2010
Received in revised form 28 June 2010
Accepted 30 June 2010
Available online 6 July 2010

Keywords:
Amino ester hydrolase
β-Lactam antibiotics
Ampicillin

ABSTRACT

α-Amino ester hydrolases (AEH) are a small class of proteins, which are highly specific for hydrolysis or synthesis of α-amino containing amides and esters including β-lactam antibiotics such as ampicillin, amoxicillin, and cephalexin. A BLAST search revealed the sequence of a putative glutaryl 7-aminocephalosporanic acid (GL-7-ACA) acylase 93% identical to a known AEH from *Xanthomonas citri*. The gene, termed *gaa*, was cloned from the genomic DNA of *Xanthomonas campestris pv. campestris* sp. strain ATCC 33913 and the corresponding protein was expressed into *Escherichia coli*. The purified protein was able to perform both hydrolysis and synthesis of a variety of α-amino β-lactam antibiotics including *(R)*-ampicillin and cephalexin, with optimal ampicillin hydrolytic activity at 25 °C and pH 6.8, with kinetic parameters of k_{cat} of 72.5 s^{-1} and K_M of 1.1 mM. The synthesis parameters α, β_o, and γ for ampicillin, determined here first for this class of proteins, are $\alpha = 0.25$, $\beta_o = 42.8\ M^{-1}$, and $\gamma = 0.23$, and demonstrate the excellent synthetic potential of these enzymes. An extensive study of site-directed mutations around the binding pocket of *X. campestris pv. campestris* AEH strongly suggests that mutation of almost any first-shell amino acid residues around the active site leads to inactive enzyme, including Y82, Y175, D207, D208, W209, Y222, and E309, in addition to those residues forming the catalytic triad, S174, H340, and D307.

1. Introduction

Semi-synthetic β-lactam antibiotics (mostly penicillins and cephalosporins) make up approximately 65% of the total world market of $15 billion for antibiotics [1]. One of the most efficient ways to produce semi-synthetic β-lactam antibiotics is via biocatalytic acylation of a β-lactam moiety, for example 6-aminopenicillanic acid (6-APA), with an activated carboxylic acid, for example (*R*)-phenylglycine methyl ester ((*R*)-PGME), as shown in Scheme 1. DSM Anti-Infectives BV (Delft, Netherlands) currently manufactures amoxicillin, cephalexin, and cefadroxil with an enzymatic process that utilizes penicillin G acylase (PGA, EC 3.5.1.11) [2]. Improved enzymatic production processes lead to lower cost and more environmentally benign production of semi-synthetic antibiotics when compared to traditional chemical synthesis [1,3–10] and the existing enzymatic synthesis.

α-Amino ester hydrolase (AEH) catalyzes the synthesis and hydrolysis of esters and amides of α-amino acids, and can be used as an alternative to the industrially employed penicillin G acylase for the synthesis and hydrolysis of α-amino containing antibiotics. While already discovered in 1974 by Takahashi et al. [11], AEHs from both *Acetobacter turbidans* (ATCC 9325) and *Xanthomonas citri* (IFO 3835) have only recently been cloned, overexpressed in *Escherichia coli*, crystallized [5,9,10], and characterized as to substrate specificity. These enzymes are serine hydrolases with a classical Ser-His-Asp catalytic triad and belong to the structural type of α/β-hydrolases [6,9,10]. The AEHs are unique in their specificity toward α-amino groups; this specificity has been associated with an acidic carboxylate cluster (D208, E309, D310) in the enzyme's active site. The current understanding of the carboxylate cluster focuses on its involvement in the recognition of the α-amino group on the substrate, thus positioning the substrate for catalysis [5]. Since only two AEHs have been fully characterized so far, it is of interest to further expand the number of characterized species in this class to enable combinatorial or data-driven protein engineering techniques such as gene recombination [12,13], combinatorial active-site saturation testing (CASTing) [14–16], or the consensus approach [17] to improve properties of these enzymes, such as thermostability, enantioselectivity, and substrate specificity. Such protein engineering techniques require multiple functional and

* Corresponding author at: School of Chemical and Biomolecular Engineering and School of Chemistry and Biochemistry, Parker H. Petit Institute for Bioengineering and Bioscience, Georgia Institute of Technology, 315 Ferst Drive, Atlanta, GA 30332-0363, USA. Fax: +1 404 894 2291.
E-mail address: andreas.bommarius@chbe.gatech.edu (A.S. Bommarius).

1381-1177/$ – see front matter © 2010 Elsevier B.V. All rights reserved.
doi:10.1016/j.molcatb.2010.06.014

Nomenclature

α	selectivity enzyme for the antibiotic substrate relative to the acyl donor
β_o	delimits the synthesis/hydrolysis ratio at low nucleophile concentrations, mM
γ	delimits the hydrolysis/synthesis ratio at the transformation of an acyl enzyme–nucleophile complex
α_{CD}	fraction of unfolded enzyme
k_{cat}	first order catalytic rate constant, s^{-1}
K_M	Michaelis constant, mM
$T_{50}{}^{30}$	temperature at which the enzyme half-life is 30 min, °C
ΔH_d	enthalpy of deactivation, kJ mol^{-1}
A	arrhenius pre-exponential factor, s^{-1}
Ea	activation energy, kJ mol^{-1}
Ed	deactivation energy, kJ mol^{-1}
T_m	temperature of melting, °C
kDa	kilodalton
E_{app}	apparent enantiomeric ratio
e.e.$_p$	enantiomeric excess of the ampicillin product

fully characterized sequences to be fully efficient. Incidentally, *X. citri* is inaccessible in the United States as it is regulated as a plant pathogen causing citrus canker in citrus plants [18], while its cousin *Xanthomonas campestris pv. campestris* is available in the ATCC as ATCC 33913.

In this investigation, the putative glutaryl 7-aminocephalosporanic acid (GL-7-ACA) acylase from *X. campestris pv. campestris* (*gaa*) (GI:21113373) was selected for characterization. The *gaa* gene was previously identified in a genome study of *X. campestris pv. campestris* [19]; however, the gene has not been previously isolated nor has the protein been tested for activity. The *gaa* gene has a high level of nucleotide alignment (89%) and the protein features a high level of amino acid identity (93%) with AEH from *X. citri* [5]. All key catalytic residues are conserved, including the catalytic triad, carboxylate cluster, and oxyanion hole (see Supplemental Materials for BLAST and CLUSTAL W alignment).

In this work, we describe the isolation and cloning of the gene from genomic DNA, as well as expression and extensive characterization of the putative 7-ACA acylase from *X. campestris pv. campestris*. We successfully produce active AEH in *E. coli* and report substrate range, kinetic and thermodynamic properties, such as half-life $\tau_{1/2}$, melting temperature T_m, and the temperature of half-residual activity at 30 min $T_{50}{}^{30}$ of the purified recombinant protein. We study the role of the acidic carboxylate cluster through alanine replacement of the active-site residues. Additionally, we evaluate the enzyme's mutability around the active site through site-directed mutations of residues within 5 Å from the ligand.

Lastly, AEH from *X. campestris pv. campestris* was employed to catalyze the kinetically controlled synthesis of the β-lactam antibiotic ampicillin as shown in Scheme 1. Such a kinetically controlled synthesis raises the issue of selectivity of synthesis versus the two competing hydrolysis reactions, primary hydrolysis of *(R)*-phenylglycine methyl ester (*(R)*-PGME) and secondary hydrolysis of ampicillin [3,6,20]. The optimal operating point is reached at the time point of maximum synthesis product concentration, $[P]_{max}$. We determine the synthesis parameters α, β_o, and γ, which can be used to predict the maximum product yield as defined by Eqs. (1)–(3) [21–23].

$$\frac{d[P_s]}{d[P_h]} = \frac{\beta_o[6-\text{APA}][(R)-\text{PGME}] - \alpha[P_s(1+\beta_o\gamma[6-\text{APA}])}{(1+\beta_o\gamma[6-\text{APA}])([(R)-\text{PGME}]+\alpha[P_s]} \quad (1)$$

$$\alpha = \frac{(k_{cat}/K_M)_{P_s}}{(k_{cat}/K_M)_{(R)-\text{PGME}}} \quad (2)$$

$$\frac{\nu_{P_s}}{\nu_{P_h}} = \frac{1}{\gamma}\left(\frac{[6-\text{APA}]}{(1/\beta_o\gamma)+[6-\text{APA}]}\right) \quad (3)$$

Here, P_s is the synthesis product ampicillin, P_h is the hydrolysis product *(R)*-phenylglycine, ν_{P_s} is the initial synthesis rate of ampicillin, and ν_{P_h} is the initial formation rate of the hydrolysis product *(R)*-phenylglycine. The differential equation (1) can be solved numerically to determine $[P]_{max}$. The Eqs. (1)–(3) have been successfully used to characterize the kinetically controlled synthesis of ampicillin [21–24].

2. Experimental

2.1. Materials

6-aminopenicillanic acid (6-APA), (*R*)-phenylglycine (*R*-PG), (*R*)-ampicillin (R-AMP), (*R*)-phenylglycine methyl ester hydrochloride ((*R*)-PGME), (*R*)-phenylglycine methyl ester hydrochloride (*S*-PGME), 7-aminocephalosporanic acid (7-ACA), 7-desacetoxycephalosporanic acid (7-ADCA), cephalexin (CEX), penicillin G (PenG) all were procured from Sigma Aldrich (St. Louis, MO). Magic Media was from Invitrogen (Carlsbad, CA), Ni-NTA Superflow Resin was from Qiagen (Germantown, MD). The

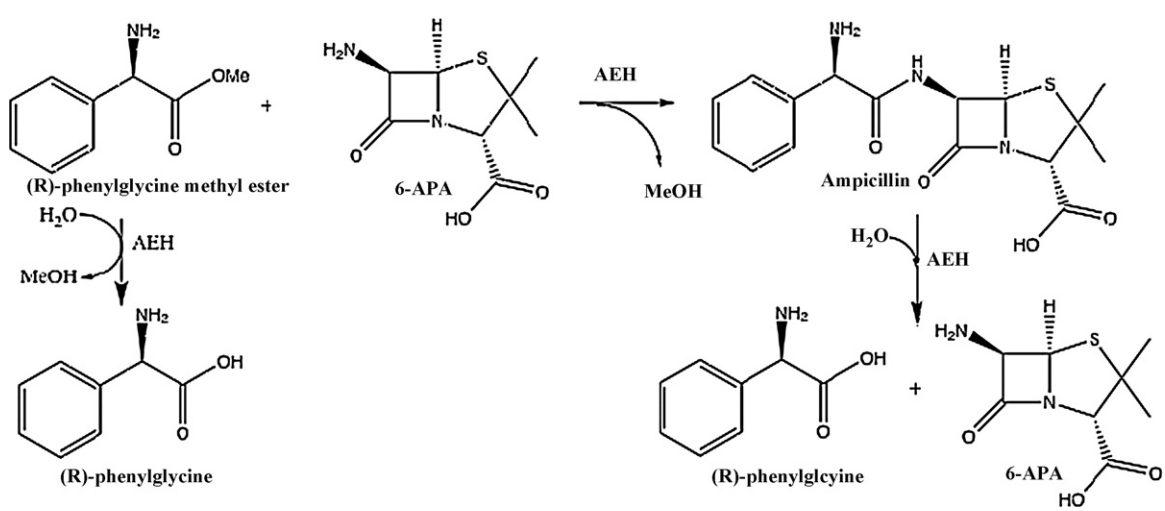

Scheme 1. Synthesis reaction of Ampicillin using AEH.

oligonuclueotides for cloning of the *gaa* gene were purchased from Eurofins-mwg|operon Biosciences (Huntsville, AL).

2.2. Bacterial strains and plasmids

The genomic DNA encoding the putative glutaryl 7-ACA acylase (*gaa*) of *Xanthomonas campestris pv. campestris* was obtained from the American Type Culture Collection (ATCC 33913D; Manassas, VA). *E. coli* strains BL21 (DE3)pLysS (Promega; Madison, WI) and XL1Blue were used for expression and cloning, respectively. The plasmid pET28a (Novagen; Darmstadt, Germany) was utilized as a cloning and expression vector containing a histidine tag (His6) for purification. All PCR reactions were performed with recombinant Pfu polymerase that was purified from *E. coli* cultivated in our lab.

2.3. DNA sequencing

The DNA sequences were determined by Eurofins-mwg|operon Biosciences (Huntsville, AL).

2.4. Cloning of gaa into expression host

For expression of the *gaa* gene in *E. coli*, the vector pETXCC (*gaa* cloned in pET28) was constructed. Primers were first used to isolate the *gaa* gene from the ATCC 33913 DNA, Forward primer 5′-CGCAGTGGCTGGAAGA CATAT-3′ and Reverse primer 5′-ATCACCGCAACCACGACCTTTGAC-3′ were used. Forward primer 5′-TGCATGCATGCCATGGTTATGCGTCGTCTT GCCGCCTGC-3′ and reverse primer 5′-CGGCGGCCCAAGCTTTCAACGC ACCGGCAGACTGATG-3′ with restriction sites Nco I and Hind III, underlined, were used to incorporate the *gaa* gene into a pET 28 vector system. A second reverse primer 5′-CGGCGGCCCAAGCTTACGCACGGCAGACTGATGTAG-3′ was used to incorporate the C-terminal 6X his tag in the pET 28 vector for ease of purification. After denaturation of the DNA, the amplifications were completed in 30 cycles of 30 s at 98 °C, 1 min at 52 °C, and 4 min at 72 °C. Products and vector were digested with NcoI and HindIII and ligated. The ligation mixture was used to transform chemically competent *E. coli* BL21(DE3)pLysS (Cm_r). The construct was confirmed by sequencing.

2.5. Site-directed mutagenesis

Variants D208A, E309A, and D310A and double and triple mutants E209A/D310A, D208A/E309A/D310A were generated using overlap PCR and ligated into the pET 28 vector system. All constructs were confirmed by sequencing. Other active-site variants were made using the QuikChange® approach.

2.6. Recombinant overexpression of the AEH

A 5-mL culture was inoculated with a single colony, grown overnight (15 mL test tubes, 30 °C, 250 rpm) and subcultured into (1:40 [v:v]) in Invitrogen MagicMedia™ (Carlsbad, CA) *E. coli* expression medium supplemented with 30 μg/mL kanamycin, 30 μg/mL chloramphenicol (Cm) (shake flask with baffles, 30 °C, 200 rpm). After 6 h, the cells were incubated for 24 h at 25 °C.

2.7. Isolation of recombinant putative glutaryl 7-ACA acylase (gaa) from E. coli

The cells were harvested by centrifugation and resuspended in 15 mL of cold lysis buffer (50 mM potassium phosphate (pH 8.0), 10 mM imidazole, and 300 mM sodium chloride) per 1 g of wet cell weight. The clarified cell lysate had a specific activity of 1.6 U/mg (total 103 U). The mixture was then sonicated and batch-purified as per the Ni-NTA His-Bind resin protocol under native conditions. Next, the pure protein was dialyzed using a Spectra/Por molecular porous membrane 12–14,000 kDa MWCO in 50 mM phosphate buffer pH 7.0. The purified enzyme had a specific activity of 59.7 U/mg (total 89.5 U), which resulted in an overall 87% yield of activity for the desired protein. The purified enzyme was analyzed using 12.5% sodium dodecylsulfate-polyacrylamide gel electrophoresis (SDS-PAGE) loaded with 15 μg of protein per lane.

2.8. Enzyme assays and determination of kinetic constants

Activity of the enzyme was assayed at 25 °C by following the hydrolysis of 20 mM ampicillin in 100 mM phosphate pH 7.0 by high performance liquid chromatography (HPLC). Before analysis, the samples were quenched and diluted 10-fold by the addition of HPLC eluent (5 mM phosphate buffer (pH 3), 300 mg/L sodium dodecylsulfate (SDS), 30% acetonitrile). The initial rates (<10% conversion) of hydrolysis of all substrates were determined by measuring product formation by HPLC. To determine kinetic parameters, the enzyme was incubated with varying substrate concentrations in the range of 0–30 mM *(R)*-ampicillin, cephalexin, and penicillin G each.

2.9. Synthesis

Synthesis of *(R)*-ampicillin and *(S)*-ampicillin was conducted at 25 °C with 60 mM *(R)*-PGME and 20 mM 6-APA in 100 mM phosphate buffer pH 6.2. A racemic mixture of 90 mM *(R/S)*-phenylglycine methyl ester hydrochloride was prepared to determine the enantioselectivity of the reaction. Lastly, synthesis of cephalexin was performed at 25 °C with 60 mM *(R)*-PGME and 20 mM 7-ADCA. Before analysis the samples were quenched and diluted 10-fold by the addition of HPLC eluent. The analysis was conducted with HPLC.

2.10. HPLC analysis

All analysis was conducted using high performance liquid chromatography complete with a Shimadzu-LC-20AT pump, Beckman Coulter Ultrasphere ODS 4.6 mm × 25 cm column, and SPD-M20A prominence diode array detector (PDA) monitored at 215 nm. The mobile phase is isocratic at 1.0 mL/min and contains 30% acetonitrile and 70% 5 mM phosphate buffer with 300 mg/L sodium dodecylsulfate (SDS) (pH 3), method adapted from Gabor and Janssen [24]. All components, *(R)*-PG, *(R)*-PG, 6-APA, *(R)*-PGME, (*S*)-PGME, *(R)*-ampicillin, *(S)*-ampicillin, analyzed on the HPLC with >95% mass balance closure. The *(R)*-ampicillin and *(S)*-ampicillin diastereomeres can be separated on the HPLC, however, the stereoisomers of RPG/SPG and *(R)*-PGME/*(S)*-PGME co-eluted. Enantiopurity of the product ($e.e._p$) was determined using the *(R)*-Amp and *(S)*-Amp concentrations.

2.11. Circular dichroism (CD)

All analysis was conducted using a JASCO CD J-810 with quartz cuvettes. Thermal scans ranged between 5 and 95 °C with a scan rate of 1 °C/min. Data was analyzed to determine ΔH and T_m as described in Greenfield [25].

3. Results and discussion

3.1. Cloning, expression, and purification

The complete 1914 bp *gaa* gene of *X. campestris pv. campestris* was isolated from the genomic DNA via PCR with primers just outside of the desired gene. The gene was cloned into pET28 with

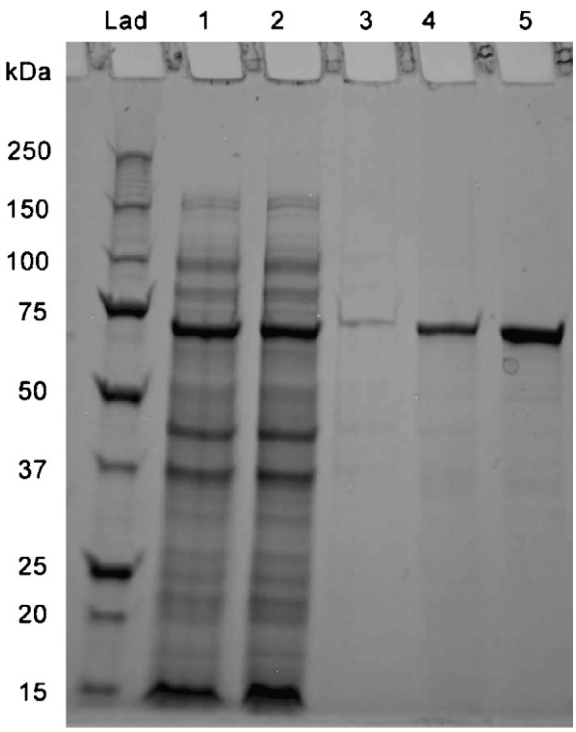

Fig. 1. Protein gel of the expressed AEH protein from *X. campestris pv. campestris*. Lane 1: pETXccH protein lysate, Lane 2: pETXccH unbound fraction, Lane 3: pETXccH Wash 1, Lane 4: pETXccH Wash 2, Lane 5: pETXccH eluent. The desired protein band is approximately 68 kDa.

and without the C-terminal 6X histidine tag, resulting in an active construct that is designated pETXcc and pETXccH, respectively, as described in Section 2 . The gene encodes a 637 amino acid polypeptide; the gene sequence was confirmed by DNA sequencing. The first 22 amino acids encode a signal peptide as predicted by the SignalP 3.0 Server [26], thus resulting in an active peptide subunit of 615 amino acids and a calculated molecular weight of 68 kDa. These constructs were transformed into *E. coli* BL21(DE3)pLysS cells. Overall expression is 3% of the total soluble protein content, similar to expression levels previously reported for AEHs [5,6,9]. Activities of soluble lysate from pETXcc and pETXccH were compared indicating that the histidine tag did not impact expression of the plasmid, confirming previous work on the AEH from *A. turbidans* [5,6,9]. Pure protein was obtained through immobilized metal ion affinity chromatography IMAC purification on Ni-NTA of pETXccH as described in Section 2. The SDS-PAGE protein band at 68 kDa is the desired AEH protein (Fig. 1).

3.2. Hydrolysis kinetics

The AEH family is specific for esters and amides bearing an α-amino group, however, it is able to accept both cephalosporins and penicillins as the β-lactam moiety. For this reason, a range of substrates that include these combinations was tested under hydrolysis conditions. The results are summarized in Table 1. Indeed, our protein from *X. campestris* is active only on α-amino containing β-lactam antibiotics and as thus did not accept penicillin G. The k_{cat} and K_M values of ampicillin hydrolysis at 25 °C and pH 6.8 were 72.5 s^{-1} and 1.1 mM, respectively.

3.3. pH and temperature optima

The hydrolysis activity of AEH on ampicillin as a function of the pH value and buffer system was studied between pH 4 and 10; an optimum pH of 6.8 was found (Supplemental Fig. S-1). Fig. 2A illustrates the temperature dependence of the AEH activity for the hydrolysis of ampicillin. The optimum temperature was found to be 25 °C. Between 6 and 25 °C, the activity increased with an activation energy of 56.7 kJ mol^{-1} (see Supplemental Material for Arrhenius fits). CD scans (Fig. 2B) were performed on the pure protein to determine the melting temperature (α_{CD} = 0.5) of the protein. Using a two-state model, the melting temperature T_m was determined to be 32.4 °C, the enthalpy of deactivation ΔH_d was calculated with residual activity data between 25 and 40 °C to be 174 kJ mol^{-1} (R^2 of 0.99). The protein was also evaluated by incubating at a range of temperatures for 30 min, resulting in a $T_{50}{}^{30}$ value of 27 ± 2 °C, further illustrating that the enzyme is not very thermostable (Fig. 2C). As the rate of deactivation is not clearly first order at 30 °C, we just report the observed half-life of the protein: 5 min (Fig. 2D). This low thermostability potentially can be associated with subunit dissociation [27,28]. Additionally, it is likely that the low thermostability of this protein hinders the ability for the protein to tolerate mutations, which tend to further decrease thermostability, as suggested by both Tokuriki and Tawfik [30] and Bloom and Arnold [29]. Furthermore, the deactivation and unfolding both occur in a broad temperature range between 25 and 40 °C, indicating that the protein unfolds in a fairly non-cooperative manner.

Table 1
Kinetic constants for the AEH from *X. campestris pv. campestris*.[a].

Substrate	k_{cat} (s^{-1})	K_M (mM)	k_{cat}/K_M (s^{-1} mM^{-1})
(R)-ampicillin	72.5	1.1	64.5
Penicillin G	n.d.[b]	n.d.[b]	n.d.[b]
Cephalexin	200	2.2	95
(R)-PGME	982	3.7	265

[a] All reactions performed at 25 °C and pH 7, as described in Section 2.
[b] n.d., not detected.

3.4. Mutability of active site and surrounding residues

The residues of the carboxylate cluster (Fig. 3A) were each mutated to alanine (D208A, E309A, D310A). Additionally, the double mutant (E309A/D310A) and triple mutant (D208A/E309A/D310A) were constructed. These mutants were all successfully expressed in BL21(DE3)pLysS as observed by overexpression of soluble protein (SDS-PAGE gels not shown). The single variants D208A and E309A both destroyed 100% of the wild-type (WT) activity toward ampicillin and cephalexin, and variant D310A reached only 4% ampicillin conversion after 24 h of incubation at 25 °C. Both the double mutant and triple mutant resulted in no detectable activity. Despite replacing all three residues that are required for recognition of the α-amino group on ampicillin with alanine, none of the mutants showed activity toward penicillin G, which lacks the α-amino group, thus indicating that the carboxylate cluster residues are critical for both the activity and substrate specificity of this enzyme.

Additional single point mutations were constructed around the active site of the enzyme: Y82A, S174A, Y175 (A,R,D,C,H,L,S,V), D207(A,L,N), D208(L,N), W209A, Y222A, D307N, E309(L,Q), and D310(L,N). These residues are all within 5 Å of the active site. S174, D307, H340 (not mutated) form the catalytic triad, Y82A, Y175A are part of the oxyanion hole, and D208, E309, D310 form the carboxylate cluster. Barends et al. found that a mutation at position Y206A (AEH from *X. campestris pv. campestris* residue Y175A) decreased the enzyme activity but led to improved synthesis properties [6]. The functions of W209 and Y222 are unknown, but are expected to provide bulk to the enzyme pocket and be involved in pi–pi stacking with the substrate. It was expected that some of these mutations would dramatically affect the enzyme activity; however, previous

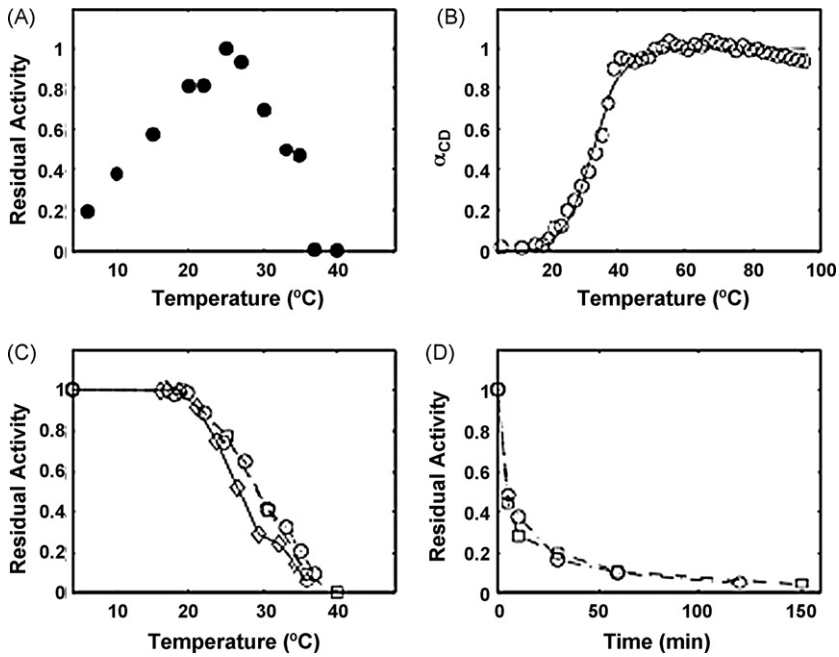

Fig. 2. (A) The temperature profile for the hydrolysis of ampicillin using the AEH from *X. campestris pv. campestris*. An Arrhenius fit of the temperature activation energy (E_a = 57 kJ mol^{-1}, A = 7.3E+11 s^{-1}, R^2 = 0.95) and deactivation constants (E_d = −82 kJ mol^{-1}, A = 3.4E−14 s^{-1}, R^2 = 1.0). Only the first four deactivation points were considered in the fit, initial activity at >35 °C is difficult to quantify since the deactivation occurs in <1 min. (B) CD thermal scan result fit to a two-state deactivation model, resulting in a calculated T_m = 32.4 °C. (C) Residual activity of AEH after incubation at reported temperature for 30 min, protein was immediately quenched on ice prior to determining residual activity at 25 °C as described in Section 2. (D) Residual activity at 25 °C of AEH after incubation at 30 °C at reported time.

work with serine hydrolases suggest that only the mutations on the catalytic serine, S174, and histidine, H340, should destroy all 100% activity of the enzyme. In contrast to expectations, with the exception of Y175A and D310N, none of the variants exhibited any ampicillin conversion after 24-h incubation at 25 °C. To test if the lack of AEH thermostability masks specificity toward the variants listed above, an additional reaction was conducted at 17 °C; higher ampicillin conversions were achieved for both Y175A (59%) and D310N (40%) after 24 h under these conditions. The other single variants still did not exhibit any conversion, thus indicating the critical nature of all of these active-site residues, including carboxylate cluster residues D208 and E309, for the activity of this enzyme.

Lastly, to investigate the role of the conserved active-site residues in homologs, we compared *X. campestris* AEH to *Rhodococcus* sp. cocaine esterase (RhCocE) [31] and J1 glutaryl 7-ACA acylase (J1) [32]. Both the RhCocE and the J1 enzyme do not require an α-amino group in the substrate (Table 2). Both the sequence and crystal structures of AEH pdb:2B4K and RhCocE pdb:1JU3 were aligned using CLUSTAL W and superimposed using PyMol (DeLano Scientific), respectively (see Supplemental Material). The PyMol alignment was anchored on the position of the catalytic triad; from this alignment the alpha carbon atoms superimposed with an RMS of 0.6 Å (Fig. 3A). In both RhCocE and J1 the catalytic triad and oxyanion hole are conserved, while different amino acid residues

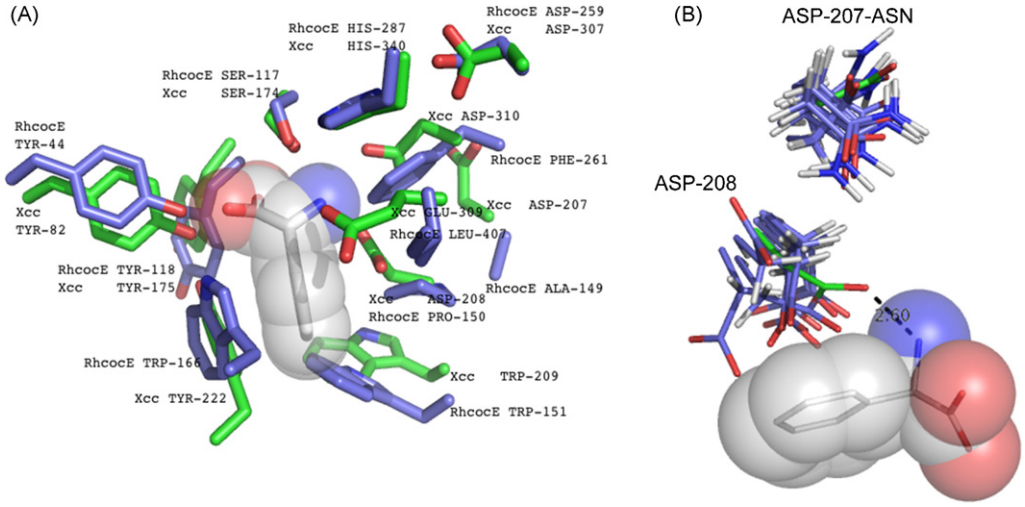

Fig. 3. A. PyMol representation of the active-site residues from the AEH from *A. turbidans* shown with *(R)*-PG bound, pdb 2b4k [22] aligned with the RhcocE. The proteins were aligned using PyMol software using the alpha carbons of the catalytic triad (Xcc SER-174, Xcc HIS-340, and Xcc ASP-307) to an RMS of 0.6 Å. The residue number reflects the numbering for *X. campestris pv. campestris (XCC)* and for the *RhcocE.* B. RosettaBackrub model [33] for mutation Asp207Asn, the top 10 structures are shown (blue) the wild-type structure is shown in green. The position of the Asp208 side chain is repositioned away from the α-amino of *(R)*-phenylglcyine, which impacts the polar interactions between *(R)*-PG and Asp208. (For interpretation of the references to colors in this figure legend, the reader is referred to the web version of this article.)

Table 2
Alignment of active-site residues of *X. campestris pv. campestris* AEH, RhCoCE, and J1 acylase.

X. campestris pv. campestris	RhCocE[a]	J1 acylase[a]	Comment
Y82	Y44	Y84	Oxyanion hole
S174	S117	S152	Active serine, catalytic triad
Y175	Y118	Y153	Oxyanion hole
D207	A149	E184	
D208	P150	V185	
W209	W151	F186	
Y222	W166[b]	W200[b]	Larger aromatic
D307	D259	D291	Catalytic triad
E309	–, L407[c]	–, T470[c]	
D310	F261	L293	
H340	H287	H336	Catalytic triad

[a] Residue numbering includes the signal sequence of both RhCocE and J1 acylase.
[b] The CLUSTAL W sequence alignment indicates that G165 and S199 should align with Y222, however, in the 3D homology model (Supplemental Material), it is clear that the residues W166 and W200 (based on homology) properly align at this site.
[c] While there is a gap in the sequence alignment, 3D alignment using PyMol indicates that these residues fill the space occupied by E309 in *X. campestris pv. campestris.*

are found at AEH positions D207, D208, W209, Y222, E309, and D310. Positions W209 and Y222 are replaced by different aromatic residues suggesting that these changes compensate for size variability in the substrate. In the sequence alignment of *X. campestris pv. campestris* AEH and RhCocE, a gap appears at the E309 position. However, in the PyMol superposition of RhCocE on AEH, it appears that loop residue RhCocE L407 or the homologous J1 T470 residue fills the corresponding space in the binding pocket with a small non-polar amino acid. At position D207, the RhCocE contains an alanine while J1 acylase contains a glutamate.

Our *X. campestris pv. campestris* AEH variants D207A, D207N, and D207L did not show significant activity toward ampicillin or cephalexin. While D207 does not directly interact with the α-amino substrate, as the γ-carbon of D207 is >4 Å from the α-amino moiety on the substrate, the side chain D207 has polar interactions with the backbone of several second-shell residues (W312, G313, I201, D202). These backbone interactions are important in the positioning of its adjacent residue D208 that interacts with the substrate as part of the carboxylate cluster. This scenario was further confirmed using a RosettaBackrub model [33] of the D207N mutation. In this model not only were the side chain to backbone interactions of D207 eliminated, the position of the γ-carbon of the D208 residue was moved 0.8–1.5 Å from the original position, which may disrupt the salt bridge formed with the substrate (Fig. 3B). These results suggest that the entire group of acidic residues near the active site, D207, as well as D208, E309, and D310, are critical for protein function.

3.5. Synthesis of ampicillin

(R)-ampicillin was synthesized through enzymatic acylation of *(R)*-PGME with 6-APA in purely aqueous system as shown in Scheme 1 and Fig. 4A. This reaction is coupled with two enzyme-catalyzed side reactions, primary hydrolysis of *(R)*-PGME to *(R)*-PG and methanol and secondary hydrolysis of *(R)*-ampicillin to *(R)*-PG and 6-APA. The results of the synthesis reaction are shown in Fig. 4. At [6-APA] = 20 mM and [*(R)*-PGME] = 60 mM, the maximum product concentration $[P]_{max}$ achieved was ~10 mM, or 50% conversion with respect to 6-APA. The reaction stalls 40 min with substrate still available: concentrations at 40 min are 10 mM (AMP), 10 mM (6-APA), 35 mM (*(R)*-PG), and 15 mM (*(R)*-PGME). Even after 24 h under these conditions the product remained in solution at 10 mM and no secondary ampicillin hydrolysis was observed. Enzyme activity has been confirmed for the duration of the synthesis; thus, the lack of conversion is not due to poor enzyme stability.

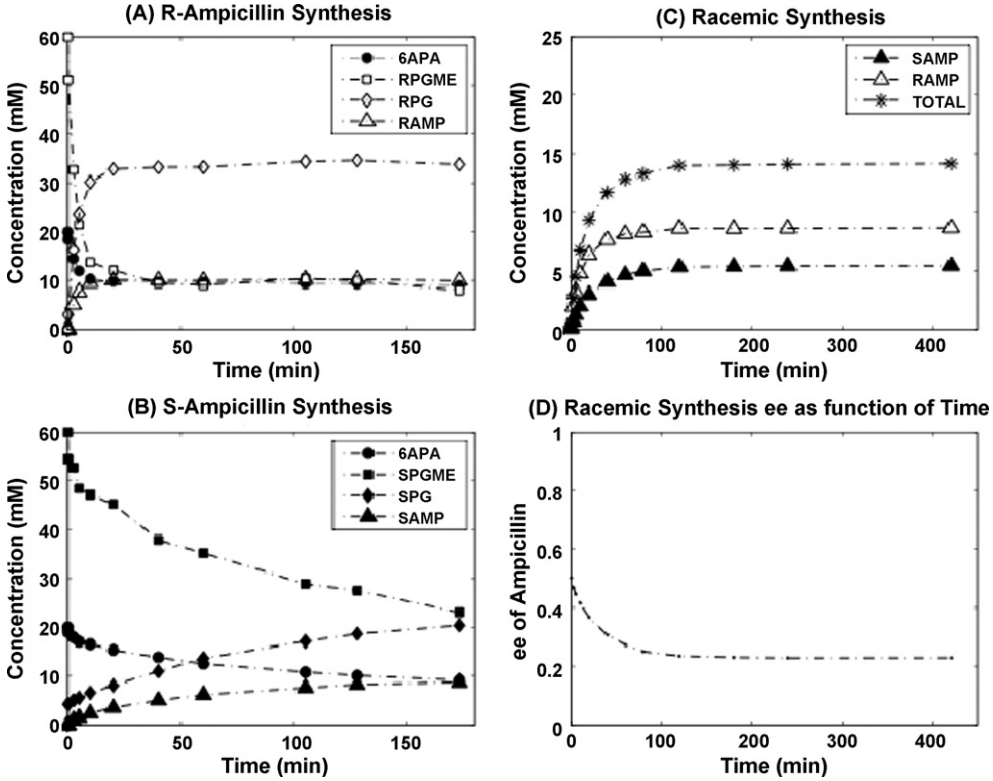

Fig. 4. (A) Kinetically controlled synthesis of *(R)*-ampicillin with AEH from *X. campestris pv. campestris* starting with 20 mM 6-APA and 60 mM R-PGME (B) Kinetically controlled synthesis of *(R)*-ampicillin employing AEH from *X. campestris pv. campestris* starting with 20 mM 6-APA and 60 mM *S*-PGME (C) Synthesis of (*R*/*S*)-ampicillin starting with 20 mM 6-APA and 90 mM racemic PGME. (D) Plot of the change in enantioselectivity of the reaction over time, when starting with racemic PGME.

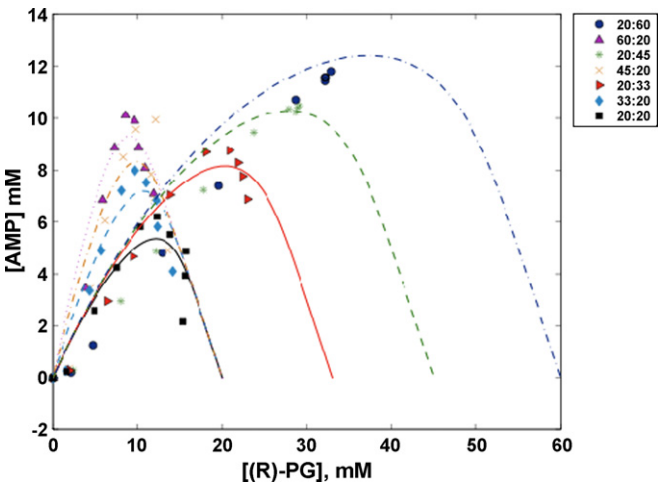

Fig. 5. Plot of [RPG] versus [AMP] results for six synthesis reactions at various $[6APA]_o$:$[RPGME]_o$ ratios and concentrations (20:20 mM, 33:20 mM, 45:20 mM, 60:20 mM, 20:33 mM; 20:45 mM; 20:60 mM), fit to the model equation (Eq. (1)) with parameters $\alpha = 0.25$, $\beta_o = 42.8\,M^{-1}$, and $\gamma = 0.23$. The experimental results are shown by the data points, while the model fits are represented by the lines.

Furthermore, secondary hydrolysis can occur when using <40 mM *(R)*-PGME as the substrate (Fig. 5). Similar results for secondary hydrolysis were obtained for cephalexin synthesis with partially pure enzyme isolated from *X. citri* (non-recombinant), when using a 20 mM (7-ADCA):60 mM (*(R)*-PGME) ratio [34]. Employing *X. campestris pv. campestris* AEH, *(S)*-ampicillin was synthesized analogously to the *(R)*-enantiomer (Fig. 4B). The initial synthesis rate of *(S)*-ampicillin was 0.31 mM min^{-1} over the linear portion of the synthesis curve, only one seventh of the *(R)*-ampicillin synthesis rate of 2.0 mM min^{-1}, indicating the enzyme's preference for the *(R)*-substrate. Enantioselectivity was also tested in the competing synthesis of both *(R)*- and *(S)*-ampicillin (Fig. 4C) employing a starting ratio of 90 mM (*(R/S)*-PGME): 20 mM (6-APA). While the enzyme has a preference for *(R)*-ampicillin, the resulting enantiomeric excess $e.e._p$ of the ampicillin product was only 22% at steady state (Fig. 4D), resulting in an apparent enantiomeric ratio E_{app} of only 2.4 (Eq. (4)). Higher overall yields were observed when starting with racemic PGME, with $[P]_{max}$ at 14 mM resulting in 70% conversion of the 6-APA substrate.

$$E_{app} = \ln\left\{\frac{1 - x(1 + e.e._p)}{1 - x(1 - e.e._p)}\right\} \quad (4)$$

where x = degree of conversion.

Kinetic parameters α, β_o and γ were determined to fully characterize the synthetic properties of this enzyme. α-Values for the synthesis of ampicillin with the wild-type AEHs range from $\alpha = 0.15–1.09$ for *A. turbidans* to $\alpha = 2.2$ for *X. citri*, calculated from previously reported data [5]. Reported α-values for the PAS2 penicillin G acylases range $\alpha = 7.6–16.4$ for *(R)*-PGME [24]. The α-value for the AEH from *X. campestris pv. campestris* was calculated from the initial hydrolysis data (Table 1) to be 0.25, at the low end of the reported range. A low α is desirable as it is an indication for the enzyme's specificity for the synthesis substrate (*(R)*-PGME) over that of the acyl donor, whereas a high α would indicate high secondary hydrolysis rate. The nucleophilic reactivity is defined by the β_o and γ values. β_o and γ were determined from a non-linear regression of a plot of $[6\text{-APA}]_o$, which ranged from 20 to 60 mM, at constant $[(R)\text{-PGME}]_o$ concentration of 20 mM, versus the initial synthesis:hydrolysis ratio observed during synthesis reactions. The parameters were calculated to be $\beta_o = 42.8\,M^{-1}$ and $\gamma = 0.23$ with an R^2 of 0.99 (see Supplemental Material). It is preferable that both β_o and $1/\gamma$ ($1/\gamma = 4.3$) values to be high [22,24] to indicate low formation of the hydrolytic by-products from both primary and secondary hydrolysis. The β_o and γ values for wild-type PGA ampicillin synthesis range from $\beta_o = 0.06$ to $0.50\,mM^{-1}$ and $1/\gamma = 6$ to 16 [23,24,35], with mutant PGA PAS2 (TM33) reported to have $\beta_o = 10.2\,mM^{-1}$ and $1/\gamma = 286$ for ampicillin synthesis [24]. To the best of our knowledge, β_o and γ values have not previously been calculated for this class of enzymes.

The kinetic parameters are able to closely estimate P_{max} when fit employing Eqs. (1)–(3) (Fig. 5). While the model appropriately tracks the raw data (Fig. 5), it should be noted that when *(R)*-PGME is in excess (20:45, 20:60) the model does not predict the lack of secondary hydrolysis when the *(R)*-PG concentration reaches ~32 mM, as observed by the clusters of points on the 20:45 and 20:60 curves. This finding suggests an inhibition effect of *(R)*-PG at this concentration.

4. Conclusions

The AEH from *X. campestris pv. campestris* strain ATCC 33913 displayed comparable levels of specific activity and improved synthetic properties compared to AEH from *X. citri* and possibly also to AEH from *A. turbidans*, as evidenced by its lower α-value, β_o and clearly favorable compared to the PGA derived enzymes, and γ values comparable to wt-PGA. The enzyme's unique ability to catalyze the β-lactam synthesis with minimal secondary hydrolysis in purely aqueous solutions renders this enzyme an even more interesting target for β-lactam synthesis. The most commonly industrially used enzyme currently employed for this reaction, penicillin G acylase (E.C. 3.5.1.11), exhibits significantly more secondary hydrolysis, unless it is reacted in a biphasic system or highly concentrated solutions [3,4,21].

The current understanding of the carboxylate cluster focuses on its involvement in the recognition of the α-amino group on the substrate, thus positioning the substrate for catalysis [5]. We argue that our results demonstrate that D207 should be regarded as part of the critical residues required for α-amino group recognition, just as D208, E309, and D310. Surprisingly, a single alanine replacement of any of the critical residues totally suppressed or at least significantly decreased the wild-type activity of the enzyme. We hypothesize that this observation is due to the need for a highly electron-deficient substrate carbonyl carbon in addition to the requirement of the α-amino group to be hydrogen-bonded to the carboxylate residues. Replacement of the negatively charged residues with alanine was insufficient to shift the substrate range to antibiotics that lack the α-amino group. We therefore conclude that the carboxylate cluster is critical for both recognition and catalysis.

We have successfully expanded the available repertoire of AEHs. The lack of mutability around the AEH active site suggest that these proteins are highly evolved for their substrate specificity toward α-amino carboxylic acid electrophiles, as there are many residues associated with its substrate specificity. The enzyme has very good synthetic properties toward the substrate and would be useful for industrial applications.

Acknowledgements

The authors gratefully acknowledge support from the National Institute of Health (Grant # 5R01AI064817-02). The authors would like to thank Dr. Javier Chaparro-Riggers, Dr. Baraheh Azizi, Dr. Mélanie Hall, Patrick Garrett, Evelina Ponizhaylo, and Michael D. Ricketts for their guidance and assistance in the preparation of this work. We also thank Prof. Dick Janssen of the University of Groningen (Groningen, Netherlands) for helpful discussions. The authors would also like to thank Aaron Engelhart in the lab of Dr. Nick Hud at Georgia Tech for help with the CD instrumentation. J.K.B. gratefully acknowledges funding by a NSF Graduate Research Fellowship.

Appendix A. Supplementary data

Supplementary data associated with this article can be found, in the online version, at doi:10.1016/j.molcatb.2010.06.014.

References

[1] R. Elander, Appl. Microbiol. Biotechnol. 61 (2003) 385–392.
[2] A.L. Deaguero, J.K. Blum, A.S. Bommarius, Wiley's Encyclopedia of Industrial Biotechnology, in: M.C. Flickinger (Ed.), Biocatalytic Synthesis of Beta-Lactam Antibiotics, 2010, pp. 535–567.
[3] W.B.L. Alkema, E. de Vries, R. Floris, D.B. Janssen, Eur. J. Biochem. 270 (2003) 3675–3683.
[4] M. Arroyo, I. de la Mata, C. Acebal, M.P. Castillon, Appl. Microbiol. Biotechnol. 60 (2003) 507–514.
[5] T.R.M. Barends, J.J. Polderman-Tijmes, P.A. Jekel, C.M.H. Hensgens, E.J. de Vries, D.B. Janssen, B.W. Dijkstra, J. Biol. Chem. 278 (2003) 23076–23084.
[6] T.R.M. Barends, J.J. Polderman-Tijmes, P.A. Jekel, C. Williams, G. Wybenga, D.B. Janssen, B.W. Dijkstra, J. Biol. Chem. 281 (2006) 5804–5810.
[7] A. Bruggink, Synthesis of Beta-Lactam Antibiotics: Chemistry, Biocatalysis & Process Integration, Kluwer Academic Publication, 2001.
[8] A. Bruggink, E.C. Roos, E. de Vroom, Org. Process Res. Dev. 2 (1998) 128–133.
[9] J.J. Polderman-Tijmes, P.A. Jekel, E.J. de Vries, A.E.J. van Merode, R. Floris, J.-M. van der Laan, T. Sonke, D.B. Janssen, Appl. Environ. Microbiol. 68 (2002) 211–218.
[10] J.J. Polderman-Tijmes, P.A. Jekel, C.M. Jeronimus-Stratingh, A.P. Bruins, J.-M. Van Der Laan, T. Sonke, D.B. Janssen, J. Biol. Chem. 277 (2002) 28474–28482.
[11] T. Takahashi, Y. Yamazaki, K. Kato, Biochem. J. 137 (1974) 497–503.
[12] L.G. Otten, C.F. Sio, J. Vrielink, R.H. Cool, W.J. Quax, J. Biol. Chem. 277 (2002) 42121–42127.
[13] J.F. Chaparro-Riggers, B.L.W. Loo, K.M. Polizzi, P.R. Gibbs, X.S. Tang, M.J. Nelson, A.S. Bommarius, BMC Biotechnol. 7 (2007).
[14] M.T. Reetz, M. Bocola, J.D. Carballeira, D. Zha, A. Vogel, Angew. Chem. Int. Ed. Engl. 44 (2005) 4192–4196.
[15] M.T. Reetz, J.D. Carballeira, Nat. Protoc. (2007).
[16] M.T. Reetz, L.-W. Wang, M. Bocola, Angew. Chem. Int. Ed. Engl. 45 (2006) 1236–1241.
[17] K.M. Polizzi, J.F. Chaparro-Riggers, E. Vazquez-Figueroa, A.S. Bommarius, Biotechnol. J. 1 (2006) 531–536.
[18] J.H. Graham, T.R. Gottwald, J. Cubero, D.S. Achor, Mol. Plant Pathol. 5 (2004) 1–15.
[19] A.C.R. da Silva, et al., Nature 417 (2002) 459–463.
[20] H.D. Jakubke, P. Kuhl, A. Könnecke, Eur. J. Appl. Microbiol. 3 (1976) 125.
[21] S.A.W. Jager, P.A. Jekel, D.B. Janssen, Enzyme Microb. Technol. 40 (2007) 1335–1344.
[22] M.I. Youshko, G.G. Chilov, T.A. Shcherbakova, V.K. Svedas, Biochim. Biophys. Acta 1599 (2002) 134–140.
[23] M.I. Youshko, L.M. van Langen, E. de Vroom, F. van Rantwijk, R.A. Sheldon, V.K. Svedas, Biotechnol. Bioeng. 78 (2002) 589–593.
[24] E.M. Gabor, D.B. Janssen, Protein Eng. Des. Sel. 17 (2004) 571–579.
[25] N.J. Greenfield, TrAC Trends Anal. Chem. 18 (1999) 236–244.
[26] J.D. Bendtsen, H. Nielsen, G. von Heijne, S. Brunak, J. Mol. Biol. 340 (2004) 783–795.
[27] V.P. Torchilin, V.S. Trubetskoy, V.G. Omelyanenko, K. Martinek, J. Mol. Catal. 19 (1983) 291–301.
[28] R. Fernandez-Lafuente, O. Hernandez-Justiz, C. Mateo, M. Terreni, J. Alonso, J.L. Garciα-Lopez, M.A. Moreno, J.M. Guisan, J. Mol. Catal. B Enzyme 11 (2001) 633–638.
[29] J.D. Bloom, F.H. Arnold, Proc. Natl. Acad. Sci. U. S. A. 106 (Suppl. 1) (2009) 9995–10000.
[30] N. Tokuriki, D.S. Tawfik, Curr. Opin. Struct. Biol. 19 (2009) 596–604.
[31] N.A. Larsen, J.M. Turner, J. Stevens, S.J. Rosser, A. Basran, R.A. Lerner, N.C. Bruce, I.A. Wilson, Nat. Struct. Biol. 9 (2002) 17–21.
[32] M.H. Yau, J. Wang, P.W. Tsang, W.P. Fong, FEBS Lett. 580 (2006) 1465–1471.
[33] F. Lauck, C.A. Smith, G.F. Friedland, E.L. Humphris, T. Kortemme, Nucleic Acids Res., (2010).
[34] C.K. Hyun, J.H. Kim, D.D.Y. Ryu, Biotechnol. Bioeng. 42 (1993) 800–806.
[35] S.A.W. Jager, I.V. Shapovalova, P.A. Jekel, W.B.L. Alkema, V.K. Svedas, D.B. Janssen, J. Biotechnol. 133 (2008) 18–26.